Supporting Information

The Realization of Both High-Performance and Enhanced Durability of Fuel Cells: Pt-Exoskeleton Structure Electrocatalysts

Ok-Hee Kim,[†] *Yoon-Hwan Cho,*[‡] *Tae-Yeol Jeon,*[§] *Jung Won Kim,*[∥] *Yong-Hun Cho,*[∥,*] *and Yung-Eun Sung*[‡,*]

[†] Department of Science, Republic of Korea Naval Academy, Jinhae-gu, Changwon 645-797, South Korea

[‡] Center for Nanoparticle Research, Institute for Basic Science (IBS), School of Chemical and Biological Engineering, Seoul National University, Seoul 151-747, South Korea

[§] Pohang Accelerator Laboratory, Pohang University of Science and Technology, Pohang 790-784, South Korea

[∥] Department of Chemical Engineering, Kangwon National University, Samcheok 245-711, South Korea

Corresponding Author

* Corresponding author. Tel: 82-2-910-5672, fax: 82-2-910-5674.
E-mail address: yhun00@kangwon.ac.kr (Y.-H. Cho)
**Co-Corresponding author. Tel: 82-2-880-1889, fax: 82-2-888-1604.
E-mail address: ysung@snu.ac.kr (Y.-E. Sung)

Supporting Figures

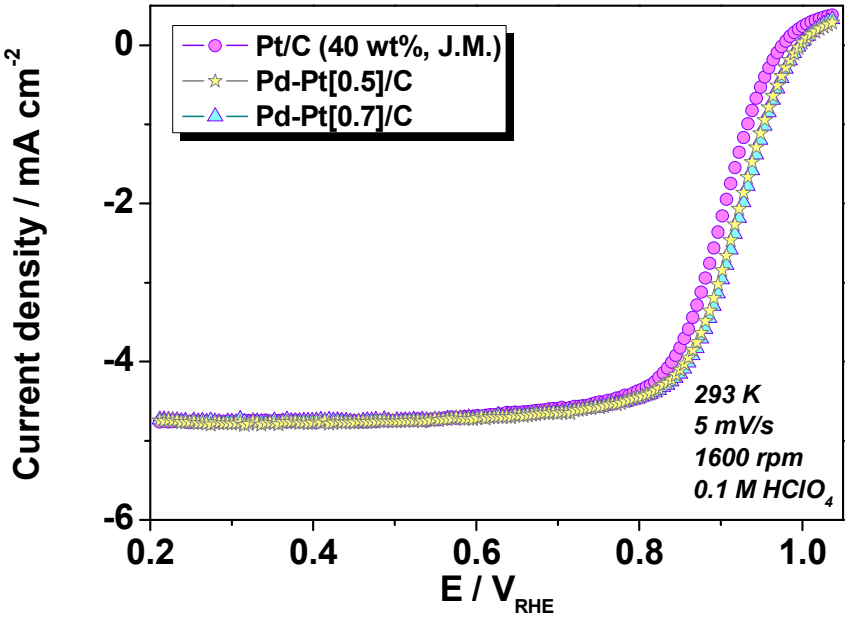

Figure S1 ORR activity of commercial Pt/C and Pd-Pt/C catalysts in half-cell. (Jeon et al. *Nanoscale*, **2012**, *4*, 6461)

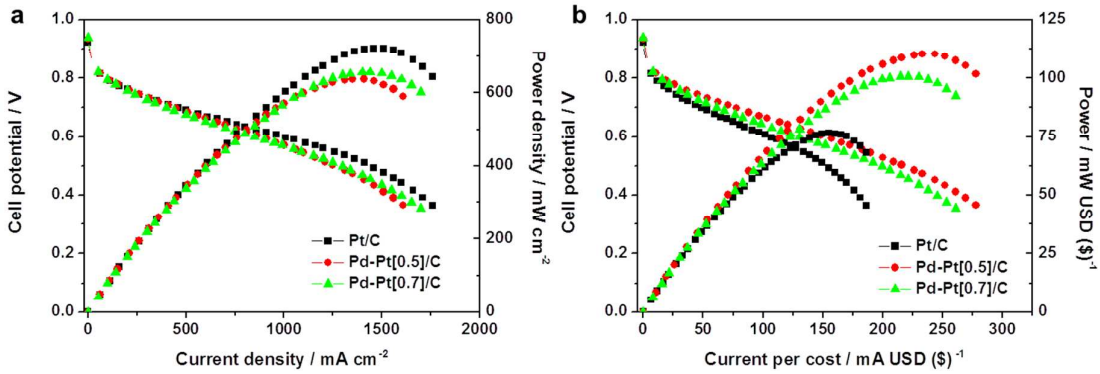

Figure S2 Polarization curves of Pd-Pt/C MEAs. a) The polarization curves normalized by active area. b) The polarization curves normalized with price of metal. Currents were normalized to the loading amount of Pt and the cost of Pt (1503 USD/Oz), Pd (866 USD/Oz). The price of metals cited from Historical London Fix price (from www. kitco.com). The cell voltages were obtained with the increasing current density using fuel cell test station to measure the current-voltage curves. Test at 70°C; fully humidified H_2/ air in MEA under atmospheric pressure

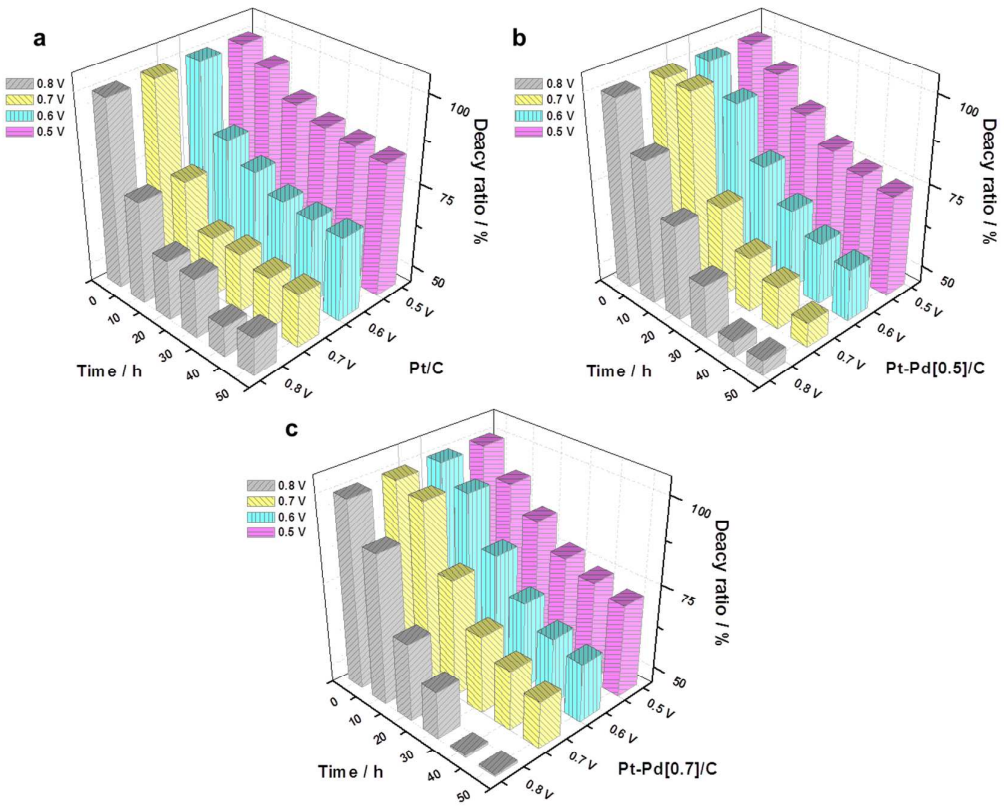

Figure S3 Degradation ratio with various voltages at the specified time intervals during ADT. a) Pt/C MEA; b) Pd-Pt[0.5]/C MEA; c) Pd-Pt[0.7]/C MEA; The ADT involved load cycling between 0.35 and OCV with a 30 sec dwell time at 70 °C, and the single cell was continuously connected with fuel cell test station during the test. The specified time intervals were 10, 20, 30, 40 and 50 h operating.

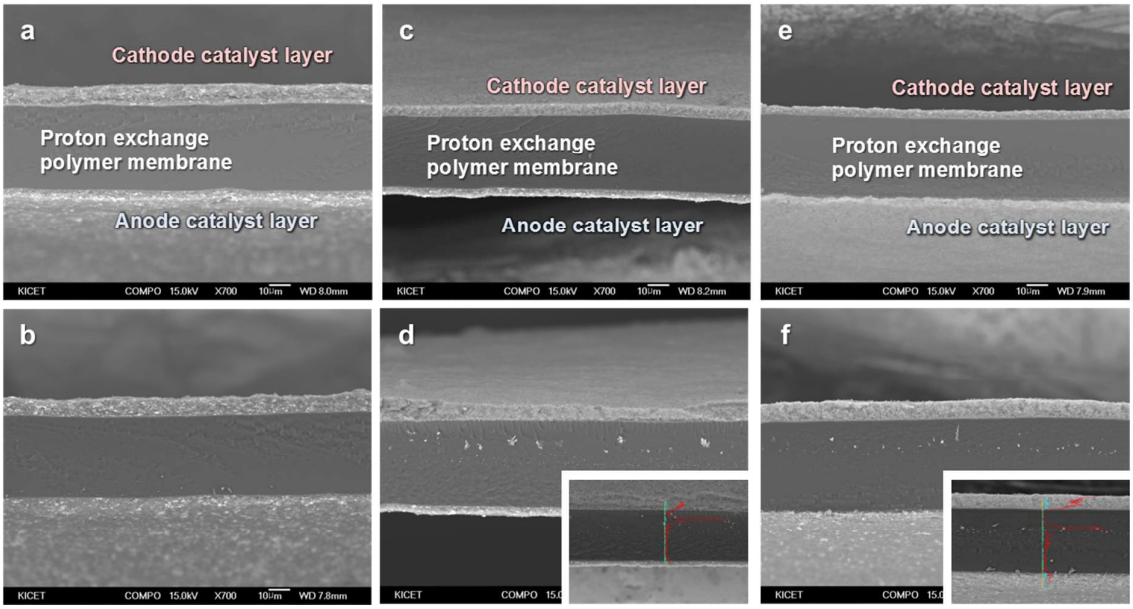

Figure S4 FE-SEM cross-section images of the MEAs before and after ADT. a) initial Pt/C MEA, b) Pt/C MEA after ADT, c) initial Pd-Pt[0.5]/C MEA, d) Pd-Pt[0.5]/C MEA after ADT, e) initial Pd-Pt[0.7]/C MEA, f) Pd-Pt[0.7]/C MEA after ADT. Inset figures of d and f are Pd elements distribution from EDX analysis.

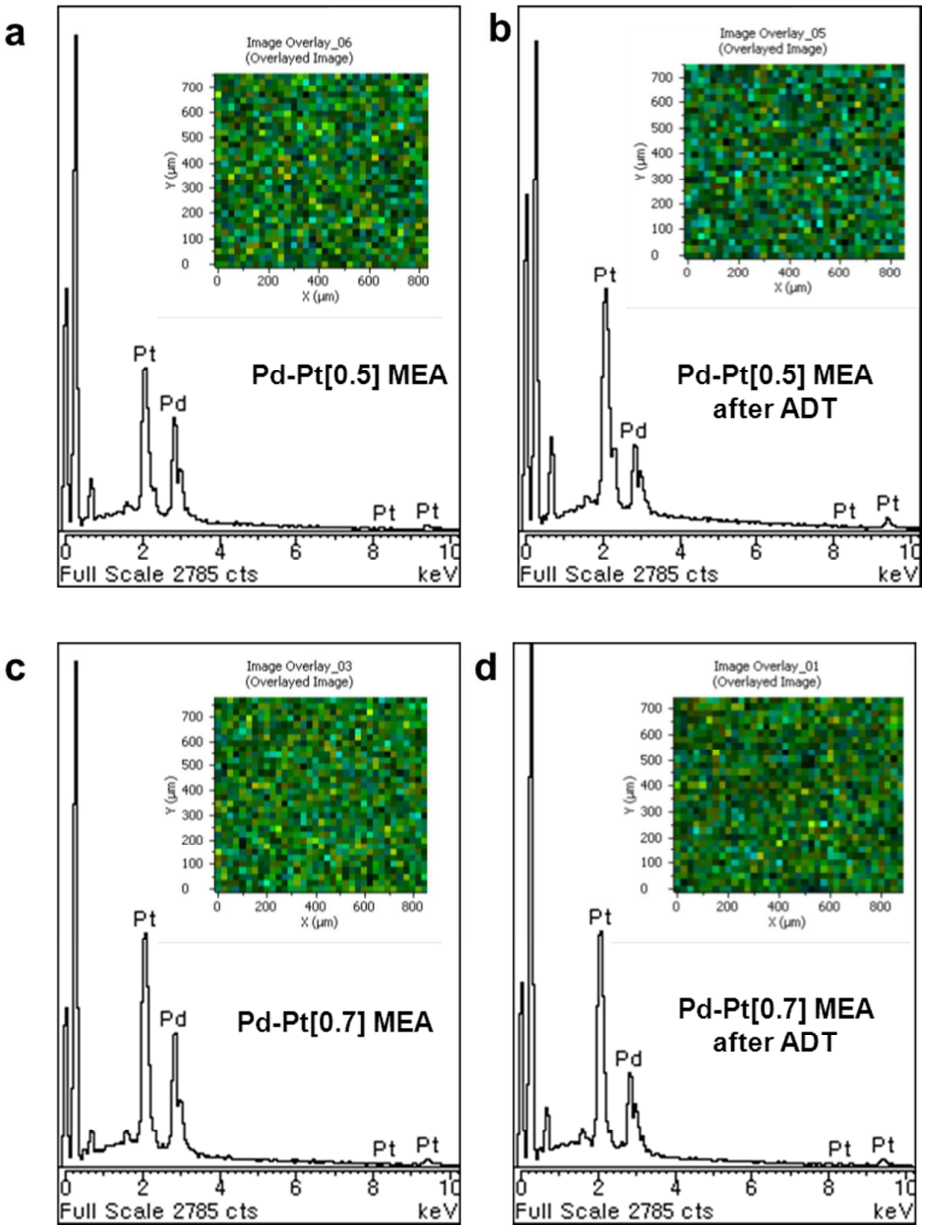

Figure S5 EDX element mapping images of the MEAs before and after ADT. a) Pd-Pt[0.5]/C MEA before ADT and b) after ADT; c) Pd-Pt[0.7]/C MEA before ADT and d) after ADT

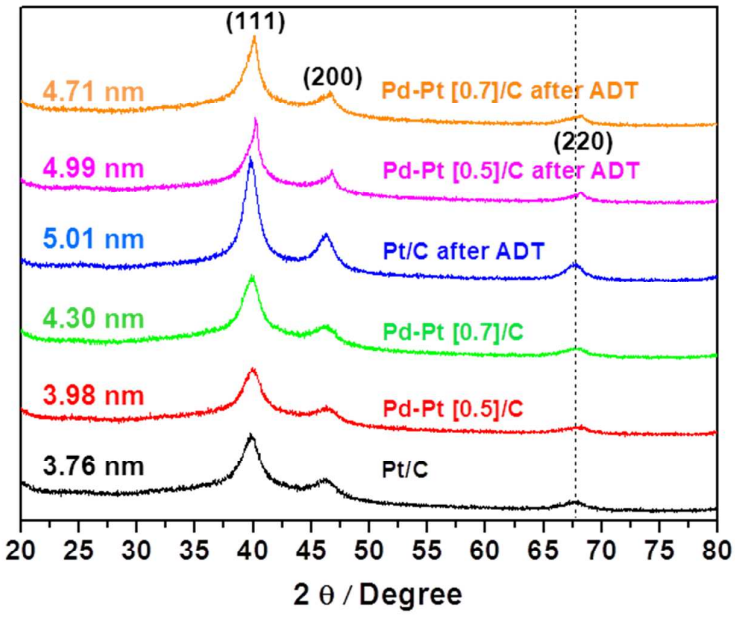

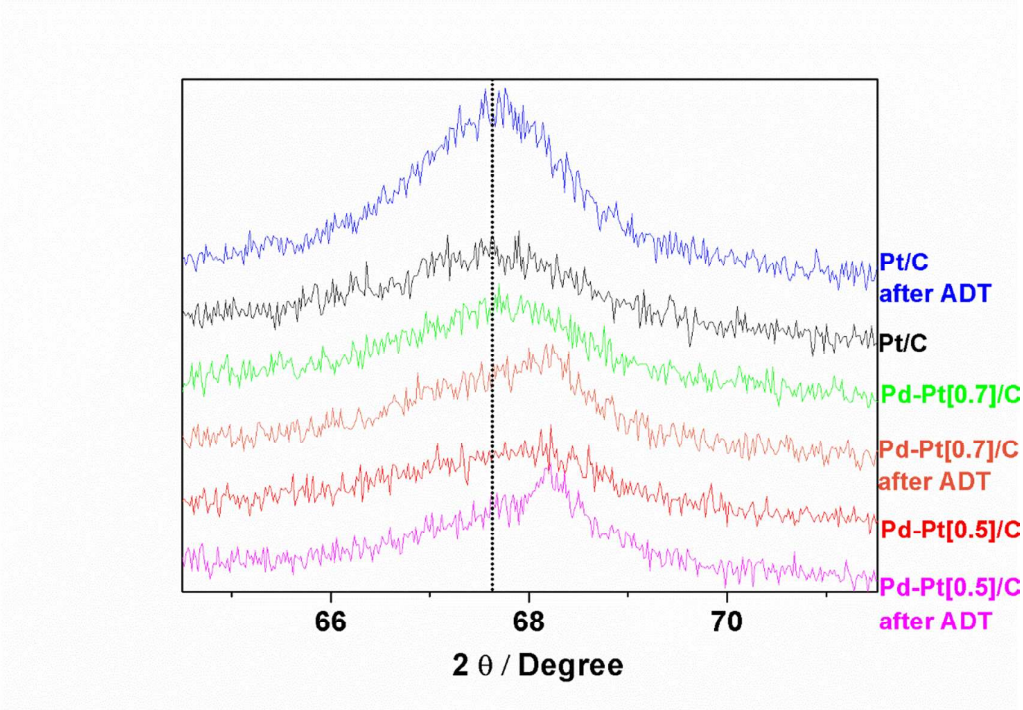

Figure S6 XRD patterns of catalyst layer before and after ADT. The (220) peak was used to calculate the average particle size of catalysts with the Scherrer equation. Detailed lines of FCC (220) peaks are at the bottom.

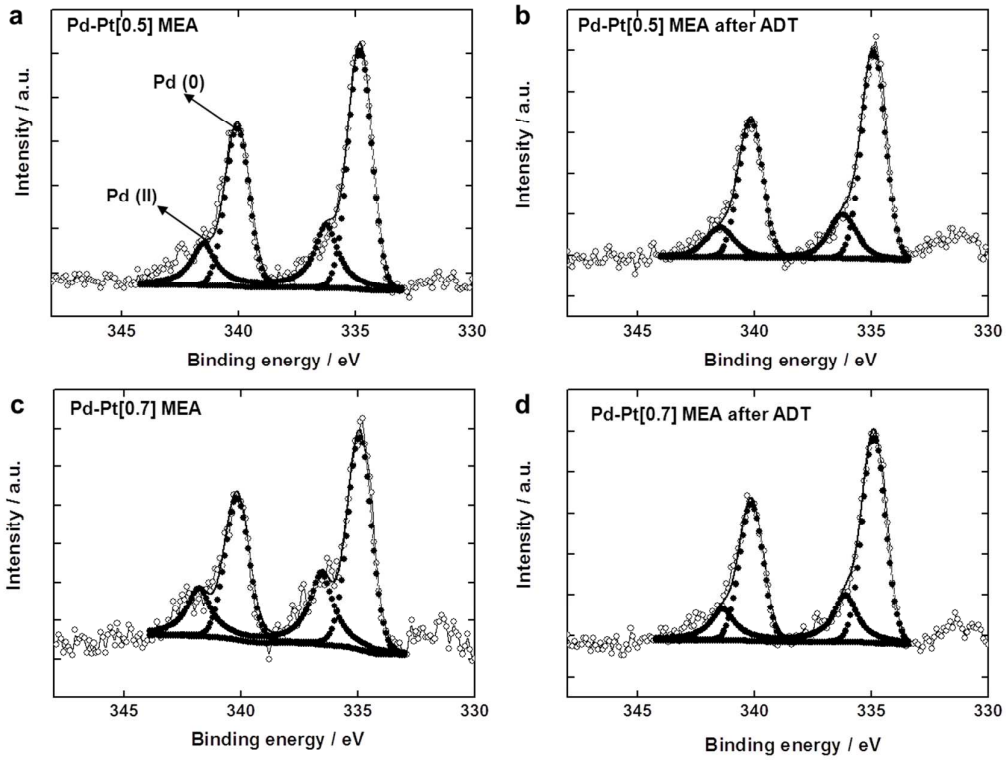

Figure S7 XPS core level spectra of Pd 3d before and after ADT. a) Pd-Pt[0.5]/C MEA before ADT and b) after ADT; c) Pd-Pt[0.7]/C MEA before ADT and d) after ADT.

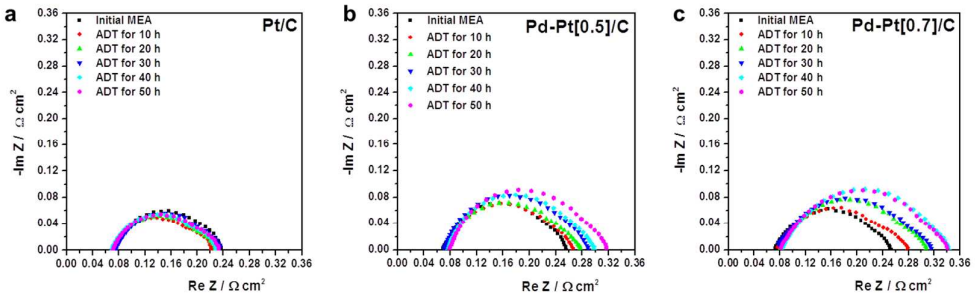

Figure S8 *in-situ* EIS of the MEAs at the specified time intervals during the ADT. a) Pt/C MEA; b) Pd-Pt[0.5]/C MEA; c) Pd-Pt[0.7]/C MEA. Those measured in time intervals (after 10, 20, 30, 40 and 50 h operating, respectively) at 0.6 V under operating conditions. In general, the charge transfer resistance is primarily determined by the interfacial reaction kinetics, ionic conductivity, and diffusion limitations within the catalyst layer. The charge transfer resistance of Pd-Pt/C was a little larger than that of commercial Pt/C, probably because of its Pd composition and undergo severe activation loss. The ohmic resistance of Pd-Pt[0.5]/C and Pd-Pt[0.7]/C slightly has increased after ADT, which means the properties of the membrane were worsened by the metal island inside.

Catalyst	Species	Binding Energy / eV	
		Before	After
Pd-Pt[0.5]/C	Pd metal ($Pd3d_{5/2}$)	340.0	340.2
	Pd metal ($Pd3d_{3/2}$)	334.8	334.9
	PdO (Ⅰ)	341.5	341.8
	PdO (Ⅱ)	336.2	336.5
Pd-Pt[0.7]/C	Pd metal ($Pd3d_{5/2}$)	340.2	340.2
	Pd metal ($Pd3d_{3/2}$)	334.9	334.9
	PdO (I)	341.5	341.5
	PdO (II)	336.2	336.2

Table S1. Binding energy of Pd oxidation states of Pd-Pt[0.5]/C and Pd-Pt[0.7]/C before/after ADT.

Supporting Note

Preparation of Ru/C and Pd/C

The catalysts were prepared aa reported in the our previous report.[1] Ru/C (21.1 wt%) was prepared via a borohydride reduction method in anhydrous ethanol. 0.25 mmol (0.08 mL) oleylamine was added to anhydrous ethanol (200 mL), and stirred for 30 min. 0.15 g of Vulcan XC-72R was added to the solution and dispersed by sonication for 40 min. After additional stirring for 30 min, ruthenium(III) chloride hydrate (0.1024 g) dissolved in anhydrous ethanol (60 mL) was added and stirred for 12 h. After sonication for 3 min, 0.49 mmol of $NaBH_4$ dissolved in 20 mL of anhydrous ethanol was quickly added to the ruthenium solution under vigorous stirring. The solution (280 mL) was stirred for 6 h, followed by filtration, washing with ethanol and drying in a vacuum oven at 40℃. Pd/C (28.4 wt%) was prepared through a similar process to the synthesis of Ru/C with the exception of using 1,2-propanediol as a solvent. Palladium(II) acetylacetonate (0.1718 g) was dissolved in 80 mL of 1,2-propanediol. This precursor solution was added to a solution composed of 1.58 mmol (0.36 mL) oleylamine, 100 mL of 1,2-propanediol, and 0.15 g of Vulcan XC-72R. This mixture solution was stirred for 12 h. After sonication for ca. 5 min, the solution was heated to 110℃ under an Ar flow and maintained at this temperature for 1 h to remove residual water. After that, 0.30 mmol of $NaBH_4$ dissolved in 20 mL of 1,2-propanediol was quickly added to the solution under vigorous stirring and maintained at this temperature for 2 h. The filtering, washing, and drying were carried out as for the Ru/C process. A heat-treatment was carried out on dried Ru/C and Pd/C samples in order to modify the particle size and to remove impurities such as dissolved carbons in the Pd lattice. The Ru/C was heat-treated for 1 h at 300℃ under Ar. For Pd/C the sample was heated to 200℃ in dry synthetic air and held at 200℃ for 1 h before being held at 200℃ for 5 min under Ar and an additional hour under Ar–H_2 (5 vol%) prior to being cooled to RT under Ar.

Pt deposition on carbon-supported metal nanoparticles

Pt deposition on the surface of the metal nanoparticles follows the same procedure as on Pd/C and Ru/C nanostructures. An appropriate amount (0.08–0.2 g) of Ru/C (or Pd/C) was dispersed in 100 mL of anhydrous ethanol and sonicated for 10 min. After additional stirring for 10 min, platinum(IV) chloride and HQ (molar ratio of HQ : $PtCl_4$ = 20 : 1) dissolved in 60 and 40 mL of anhydrous ethanol, respectively, were added to the solution containing the core materials. This solution was stirred for 1 h. After a final sonication for only 3 min, in order to avoid the reduction of Pt ions, the solution was loaded into a three-neck flask. The solution was then deaerated under Ar, heated to 70℃ at the rate of ca. 1.25℃ min^{-1} and kept for 2 h at this temperature. The solution was then cooled, filtered, washed with ethanol at room temperature, and dried at 40℃ in a vacuum oven. A control experiment was also performed by replacing Pd/C and Ru/C nanostructures by carbon black. An

appropriate amount of HQ (molar ratio of HQ : $PtCl_4$ = 20 : 1) was dissolved in a dispersion of carbon black (Vulcan XC-72R) in ethanol. To this solution an ethanol solution of platinum(IV) chloride (0.0572 g) was added. After stirring for 1 h, the solution was heated under the same conditions as for the preparation of the core–shell samples.

X-ray photoelectron spectroscopy (XPS) analysis:

Figure S6a and b shows the XPS spectra of the Pd-Pt[0.5] for the Pd3d core level spectra before and after ADT. Specific information about binding energy of each MEA was arranged in Table S1. As shown Figur. S6a and b, the spectrum could be deconvoluted into two pairs of doublets. The most intense doublet was characteristics of metallic Pd and weaker doublet could be assigned to Pd in oxidized forms. The two doublets for Pd*3d* were found at approximately 340.0 eV and 334.8 eV which corresponded to $Pd3d_{5/2}$ and $Pd3d_{3/2}$. After the ADT, the $Pd3d_{5/2}$ and $Pd3d_{3/2}$ were indicated at 340.2 eV and 334.9 eV which were similar with initial Pd-Pt[0.5]. However, the peak intensity of Pd decreased after ADT due to the Pd dissolution.

Figure S6c and d shows the XPS spectra of the Pd-Pt[0.7] before and after ADT. The binding energy of Pd in initial Pd-Pt[0.7] is similar with that of Pd-Pt[0.5]. The two doublets for Pd3d were found at approximately 340.2 eV and 334.9 eV which corresponded to $Pd3d_{5/2}$and $Pd3d_{3/2}$, respectively. After the ADT, the $Pd3d_{5/2}$ and $Pd3d_{3/2}$ were indicated at same binding energies. And the peak intensity of Pd decreased only slightly after ADT. This result indicated that the dissolution of Pd in Pd-Pt[0.7] was less than that of Pd-Pt[0.5]. The specific information about binding energy of Pd-Pt[0.7] also shown in Table S1.

In addition, the chemical composition ratios of Pd-Pt/C catalysts before and after the ADT were analyzed by XPS. As shown in Table 1, the atomic ratios of initial Pd-Pt[0.5]/C and Pd-Pt[0.7]/C were 43.82:56.18 and 35.13:64.87. This result shows different compositions from EDX analysis, because XPS result is representative of surface composition whereas EDX result represents bulk composition of catalysts. The surface composition of Pd-Pt[0.5]/C and Pd-Pt[0.7]/C catalysts show higher Pt content than the bulk composition because the catalysts are composed to Pd core and Pt shell structure. And the surface composition of Pd-Pt[0.7]/C catalysts shows higher Pt content than Pd-Pt[0.5]/C due to the different loading amount of Pt. After the ADT, the composition ratios of Pd-Pt[0.5]/C and Pd-Pt[0.7]/C catalysts were 39.19:60.81 and 33.71:66.29. The surface Pd:Pt compositions of catalyst after ADT were more Pt-rich than the bulk Pd:Pt compositions. And this result shows the dissolution of Pd takes place in the Pd-Pt core-shell catalysts. The rate of change in composition indicates that Pd-Pt[0.7]/C catalyst is more stable than Pd-Pt[0.5]/C, which is good accordance with EDX result. This result suggests that stability of Pd-Pt core-shell catalysts may be affected by the amount of Pt deposition. The dissolution of Pd core is related to the Pt shell imperfection because the dissolved Pd diffuse through the imperfection in Pt shell.[2] The Pd core in Pd-Pt[0.7] was surrounded by larger amount of the Pt shell than that of Pd-Pt[0.5]. And this may have effect on the Pt shell imperfection.

Evaluation of Pt-exoskeleton (shell) thickness:

The theoretical Pt shell thickness on Pd particle can be can be estimated by using following equation[3] (S1):

$$D_{Pt\_Pd} = D_{Pd} \times (1 + \frac{V_m(Pt)}{V_m(Pd)} \frac{[Pt]}{[Pd]})^{1/3} \qquad (S1)$$

where, D_{Pt_Pd} is the diameter of the Pd-Pt core-shell particle, D_{Pd} is the diameter of the Pd core particle (in our case is 3.75 nm), V_m is molar volume ($V_m(Pt) = 9.2498\times10^{-6}$, $V_m(Pd) = 8.8514\times10^{-6}$) and [ ] means atomic ratio of between Pt and Pd.

Theoretically, if the atomic ratio of between Pt and Pd is 0.5, then the particle size of is 4.33 nm and the thickness for the deposited Pt layer in this sample is 0.57 nm. And if the atomic ratio of between Pt and Pd is 0.7 then the particle size of is 4.52 nm and the thickness is 0.76 nm. If the 3.75 nm sized core Pd particles are completely covered with a monoatomic layer of Pt, then the thickness is equivalent to the diameter of a Pt atom (0.36 nm, considering adsorbed anions[4]) and the atomic ratio Pt between Pd should be 0.3.

However, experimental value is different from theoretical value. The result was summarized in following table. Actual Pt thickness is thinner than theoretical value. That mean the defect or extra Pt could be exist on the surface of Pd.

		Pd-Pt[0.3]	**Pd-Pt[0.5]**	**Pd-Pt[0.7]**
Theoretical	Pd-Pt particle diameter [nm]	4.12	4.33	4.52
	Pt shell thickness [nm]	0.36 (monolayer)	0.57	0.76
Experimental	Pd-Pt particle diameter [nm]	-	3.98	4.30
	Pt shell thickness [nm]	-	0.22	0.54

Table S2. Theoretical and experimental Pt thickness of Pd-Pt nanoparticle.

References

1. Jeon, T.-Y.; Pinna, N.; Yoo, S. J.; Ahn, D.; Choi, S. H.; Willinger, M.-G.; Cho, Y.-H.; Lee, K.-S.; Park, H.-Y.; Yu, S.-H.; Sung, Y-E. Selective Deposition of Pt onto Supported Metal Clusters for Fuel Cell Electrocatalysts. *Nanoscaale* **2012**, *4*, 6461–6469.

2. Sasaki, K.; Naohara, H.; Cai, Y.; Choi, Y. M.; Liu, P.; Vukmirovic, M. B.; Wang, J. X.; Adzic, R. R. Core-Protected Platinum Monolayer Shell High Stability Electrocatalysts for Fuel Cell Cathodes. *Angew. Chem. Int. Ed*. **2010**, *49,* 8602–8607
3. Zhao, D. and Xu, B.-Q. Enhancement Of Pt Utilization In Electrocatalysts by Using Gold Nanoparticles. *Angew. Chem. Int. Ed*. **2006**, *45*, 4955–4959.
4. Lide, D. R. *CRC Handbook of Chemistry and Physics*, (84th ed., CRC, Boca Raton, 2003).